Tension on kinetochore substrates is insufficient to prevent Aurora-triggered detachment

Anna K. de Regt[1], Charles L. Asbury[2*], Sue Biggins[1,3*]

[1]Basic Sciences Division and [3]Howard Hughes Medical Institute, Fred Hutchinson Cancer Research Center, Seattle WA

[2]Department of Physiology and Biophysics, University of Washington, Seattle WA

[*]Co-corresponding authors: sbiggins@fredhutch.org; casbury@uw.edu

Introduction / Abstract

Chromosome segregation requires large macromolecular structures called kinetochores to attach dynamic microtubules from opposite spindle poles[1,2]. Attachments are made iteratively, through a trial-and-error process, and proper attachments come under tension from the pulling forces of microtubules[3,4]. However, if sister kinetochores bind microtubules from the same pole[1,2], these defective attachments lack tension and must be destabilized to give another chance for proper attachments to form. This vital error correction process requires Aurora B kinase, which phosphorylates kinetochores lacking tension to reduce their affinity for microtubules[5-11]. An unresolved question is how Aurora B distinguishes the level of tension on kinetochores. There are conflicting reports on the underlying mechanism[12-16], owing in part to the difficulties of manipulating kinetochore tension *in vivo* and distinguishing kinase from opposing phosphatase activity. To address these issues, we have reconstituted Aurora B-triggered kinetochore detachment in an *in vitro* optical trapping-based flow assay. Here, we test an outstanding model by determining whether kinetochore tension is sufficient to prevent kinase-triggered detachments. Strikingly, Aurora B detaches kinetochores from microtubules under both high and low tension, providing direct evidence that the kinase does not distinguish correct versus incorrect attachments by recognizing tension-dependent changes in the conformation of its kinetochore substrates.

Main

Aurora B is a conserved and essential mitotic kinase that ensures accurate chromosome segregation and has been implicated in oncogenesis[17-19]. It is the catalytic component of the four-protein Chromosomal Passenger Complex (CPC), which is targeted to the inner centromere via the Survivin and Borealin proteins[20,21]. The fourth member of the complex, INCENP, acts as a

scaffold and activates the kinase through its C-terminus[22-27] (Fig. 1a). Aurora B is additionally activated by autophosphorylation in *trans*, and it is thought that clustering at the inner centromere facilitates this autoactivation before a centromere-centered diffusion gradient enables access to distant outer-kinetochore substrates that contact microtubules[28]. Much work has been done to identify Aurora B phosphorylation sites on the microtubule-binding elements of the kinetochore. When purified microtubule-binding kinetochore proteins are either pre-phosphorylated by Aurora B or engineered with phosphomimetic mutations at its target sites, they exhibit weakened affinity for microtubules[8,29,30].

A major outstanding question is how Aurora B distinguishes kinetochore-microtubule attachments lacking tension from those under tension. The observation that there is an Aurora B activity gradient centered at the inner centromere led to an attractive model. According to this "spatial separation" model, outer kinetochore substrates are accessible by inner centromere-localized CPC only when a kinetochore lacks tension, but substrates become spatially distant from the kinase once they come under tension[12,13]. This was the prevailing model before it was shown that inner-centromeric localization of the CPC is dispensable for proper error correction in budding yeast, chicken, and human cells[14-16]. An alternate "substrate conformation" model, which is independent of kinase localization, proposes that conformational changes occurring when kinetochores come under tension block Aurora B phosphorylation[15,16,21,31]. Electron microscopy, fluorescence microscopy, and biochemical crosslinking studies have demonstrated that kinetochores undergo large structural changes when they come under tension, which could potentially block Aurora B phosphorylation via substrate occlusion or another mechanism[32-34]. This model is analogous to the many known instances where tension-dependent conformational

changes affect binding and regulation of protein complexes, such as with integrins[35] or mechanosensitive ion channels[36].

It has not been possible to rigorously test models for Aurora B regulation within cells for several reasons. Aurora B has additional mitotic roles, so kinase inhibition acts globally and not specifically on error correction. In addition, it is challenging to test various models *in vivo* because unattached kinetochores also lack tension, and kinetochores that make attachments quickly come under tension. Finally, the phosphorylation state of individual kinetochores *in vivo* cannot be precisely correlated with kinase activity because substrate phosphorylation represents a balance of both kinase and opposing phosphatase activity[37-40]. These challenges led us to seek a controllable *in vitro* system that mimics the turnover of kinetochore-microtubule attachments during prometaphase and allows the regulation of Aurora B in this process to be studied more directly.

We previously developed an optical trap assay that reconstitutes kinetochore-microtubule attachments under tension[41]. The kinetochores are purified from budding yeast and do not carry Aurora B^{Ipl1} because they lack some inner centromeric proteins. While we cannot test the spatial separation model with these kinetochores, they provide an opportunity to test the substrate conformation model by asking whether non-centromeric Aurora B can detach kinetochores from microtubules under high tension. For such a test, we needed kinetochores lacking all kinase activity to specifically monitor the activity of exogenous Aurora B. We previously found that purified kinetochores isolated from wild-type strains contain active Mps1 kinase[42], so we used kinetochores from an *mps1-1* strain that had been shifted to the non-permissive temperature to inactivate Mps1. Consistent with previous findings in meiotic cells[43], we found that Mps1-1 kinetochores lack co-purifying Dam1 complex (Fig. S1), but otherwise resemble wild-type purified kinetochores[42]. To

ensure there was no opposing phosphatase activity, all kinetochores were purified in the presence of irreversible phosphatase inhibitors.

We next needed a source of highly active Aurora B kinase to add to the kinetochores, so we constructed a chimeric construct that has catalytic activity but lacks the other members of the CPC, including its centromeric targeting domains (Fig. 1a). Specifically, we fused the yeast INCENP^{Sli15} activation box (residues 624-698) to the N-terminus of yeast Aurora B^{Ipl1} to create AurB*. We confirmed its activity by incubating the kinetochores with ATP-γ-^{32}P and either AurB* or a kinase-dead mutant AurB* (AurB*-KD) where the catalytic lysine had been substituted with arginine (Fig. 1b). AurB* autoactivated and efficiently phosphorylated known kinetochore substrates Ndc80, Spc105 and Dsn1[13,44,45] (Fig. 1c). The key microtubule-coupling substrate Ndc80, on which a phospho-shift could be observed, was phosphorylated to greater than 50% completion in under one minute with 0.2 μM AurB* (Fig. 1d). In contrast, there was minimal phosphorylation on kinetochores incubated with 0.2 μM AurB*-KD, even after several minutes. No phosphorylation was observed on kinetochores that had been incubated only with ATP-γ-^{32}P, confirming the lack of endogenous kinase activity. To ensure that AurB* was phosphorylating physiological sites on the purified kinetochores, we repeated the experiment using phospho-deficient kinetochores with alanine substitutions at the seven known Aurora B sites on the Ndc80 N-terminus (Ndc80-7A)[44]. Because the *ndc80-7A* and *mps1-1* mutations are synthetic lethal in yeast, we used kinetochores isolated from strains containing wild-type Mps1. Although we could then detect phosphorylation in the absence of AurB*, the phosphorylation of Ndc80 protein was clearly reduced in the phospho-deficient Ndc80-7A kinetochores when compared to wild-type, and the electrophoretic mobility of Ndc80 protein was increased (Fig. 1e). Thus, AurB* phosphorylates kinetochores on physiologically-relevant sites.

When Aurora B is downregulated in cells, erroneous attachments accumulate[5-7,46]. However, it has been difficult to establish the direct results of kinetochore phosphorylation by Aurora B. Experiments in yeast suggest that chromosomes lacking tension detach from microtubules[6], but native attachments cannot be directly visualized in these small cells. In large PtK_2 cells where attachments can be seen, Aurora B inhibitor washout led to erroneously-attached kinetochores moving to cell poles instead of being immediately detached from microtubules[7]. We therefore asked whether Aurora B is sufficient to directly detach kinetochores from microtubules *in vitro*. We polymerized fluorescently-labeled tubulin into taxol-stabilized microtubules and incubated them with purified wild-type kinetochores that were retained on beads (Fig. 2a). Because the kinetochores lack stoichiometric amounts of the Dam1 complex, an important microtubule-coupling agent, we pre-incubated them with independently-purified native Dam1 complex[41,47]. The microtubule-bound kinetochores were then incubated with either buffer or AurB* and the quantity of bound microtubules was monitored over time. Incubating kinetochores with AurB* caused a phospho-shift in Ndc80 mobility and a decrease in bound microtubules over time, whereas both of these effects were absent in the kinetochores incubated with buffer alone (Figs. 2b and 2c). Incubation with AurB*-KD also did not cause microtubule release and pre-phosphorylation before microtubule incubation prevented microtubule binding (Figs. S2a and S2b). Previous studies suggest that AurB*-triggered microtubule release should primarily result from phosphorylation of microtubule-contacting residues on the Ndc80 and Dam1 proteins[8,30,48,49]. To confirm this, we repeated the experiment using phospho-deficient kinetochores purified from strains containing Ndc80-7A. We found that Ndc80-7A kinetochores released microtubules at a slower rate than wild-type kinetochores, but not as slowly as the no-kinase control (Figs. 2b and 2c), which confirms that these Ndc80 residues partially contributed to the release. Together, these

observations provide direct evidence that Aurora B phosphorylation is sufficient for the release of kinetochore-microtubule attachments. Interestingly, the kinetochores in these experiments are likely making side-on attachments to the microtubule lattice[41], a configuration similar to the initial attachments that form in prometaphase cells. Evidence suggests that side-on attachments in cells are immune to Aurora B error correction[50]. However, our results indicate that side-on-attached kinetochores are probably susceptible to Aurora-triggered release, suggesting that additional regulation might be required *in vivo* to protect them.

Kinetochores in cells make persistent, load-bearing attachments to dynamic microtubule tips and this arrangement is thought to be the relevant target for error correction. Therefore, we wanted to reconstitute tip-coupled kinetochores under differing amounts of tension to assay whether Aurora B phosphorylation could release these physiologically relevant attachments. We linked Mps1-1 kinetochores to polystyrene microbeads and then used an optical trap to attach the beads individually to the assembling tips of single, coverslip-anchored microtubules, as in previous work[30,41,51-53]. The rupture strength of tip-coupled Mps1-1 kinetochores was relatively low, presumably because they lack co-purifying Dam1 complex (Fig. S3a), so we again separately purified Dam1 complex and included it in the assay buffer. Tip-coupling strength was improved, and the Mps1-1 kinetochores could remain persistently attached to growing and shortening tips under a variety of tensile forces (Figs. S3a and S3b).

To test whether Aurora B could disrupt the attachments, we adapted the trapping assay to introduce AurB* into the reaction chamber by flowing in kinase-containing buffer once a tip-coupled kinetochore-microtubule attachment had been established (Fig. 3a). This approach was technically challenging. Unlike previous versions of our optical trap assay, only one kinetochore attachment could be probed per slide, because any free-floating unattached kinetochores became

phosphorylated once AurB* was introduced and thus were unsuitable for further measurements. Moreover, kinase introduction required flow in the chamber that caused extra beads to catch in the laser, which ended the events prematurely (Fig. 3b, Movie 1). To minimize the frequency of such interruptions, we kept the flowrate and the concentration of conjugated beads low, and we used the weakest possible trap stiffness (see Materials & Methods). ATP was included in the buffer before and after the exchange. Under these modified assay conditions, the tip-tracking of kinetochore beads was not detectably disturbed by the onset of flow (Figs. 3b and 3c).

To mimic erroneous attachments that should be corrected, we applied a constant low tension of ~1 pN between a kinetochore-coupled bead and a microtubule[41], introduced either AurB* or AurB*-KD, and then monitored the bead until either detachment or interruption (Fig. 4a). To avoid biasing the data towards higher detachment rates, we did not discard events that were interrupted and instead calculated overall detachment rates by dividing the number of detachments observed for a given condition by the total observation time after kinase flow was initiated. The spontaneous detachment rate in the presence of AurB*-KD was $2.3 \pm 0.9\ hr^{-1}$. When active AurB* was flowed in, the detachment rate was elevated 3-fold to $7.2 \pm 2.2\ hr^{-1}$, demonstrating that Aurora B can directly disrupt tip-coupled kinetochore-microtubule attachments (Figs. 4b and 4c, Movie 2). These data demonstrate that Aurora B activity is sufficient to directly detach kinetochores from microtubule tips *in vitro*.

We next sought to test one of the major models that has been proposed to explain the tension-dependent suppression of Aurora B activity: the substrate conformation model. To determine whether tension induces conformational changes that prevent Aurora B-mediated detachments, we put kinetochores under high tension, applying a constant force of 5 pN[41], and then flowed in either AurB* or AurB*-KD. The substrate conformation model predicts that

detachment rates should be similarly low, with either AurB* or AurB*-KD, when the attachments are held under high tension. However, high force did not prevent Aurora B-mediated detachments and AurB* was still able to robustly trigger detachments at high force (Fig. 5a-c). One explanation for these results would be that we had not applied enough tension, so we collected data up to 8 pN, where detachment rates were high even in the absence of kinase activity. However, there was not observable suppression of AurB* activity at any force (Fig. S4a). We note that while previous experiments in the absence of kinase activity have shown that tension can suppress kinetochore detachment[41,53], we did not see this effect under the conditions used here, even in the presence of only AurB*-KD (Supplementary Note). To ensure that the elevated detachment rates we observed in the presence of active AurB* were due to kinase activity, we measured detachment rates at two different concentrations of AurB*: 5 μM and 0.5 μM. At a high force where the effects of AurB* versus AurB*-KD flow were very different, detachment rates showed a clear dependence on enzyme concentration (Fig. 5b-c). These results were not artifacts of our mutant Mps1-1 kinetochores or the addition of Dam1 complex, as we also measured detachment rates of wild-type kinetochores from microtubules and found that AurB* again stimulated detachments (Fig. S4b). Together, these data strongly suggest that tension alone does not alter the ability of Aurora B to access its kinetochore substrates.

A number of models have been proposed to explain how Aurora B selectively weakens kinetochore-microtubule attachments that lack tension, while leaving load-bearing, tip-coupled kinetochores unmodified. Rigorously testing such models requires independent control of tension, attachment, and enzyme activity. Here, we developed an assay that fulfills these needs and allows components to be introduced while kinetochore-microtubule attachments are held continuously under tension. While previous work has shown that pre-phosphorylation reduces the microtubule

binding affinity of individual kinetochore components[8,29,30], our results provide the first direct demonstration that Aurora B activity is sufficient to detach kinetochores from dynamic microtubule tips. Recent work suggests that Aurora B's inner centromere localization is dispensable for error correction in cells[14-16], leading to the idea that changes in substrate conformation might be responsible for its tension-dependent activity[15,16,21,31]. However, we find that the kinase readily releases load-bearing kinetochore-microtubule attachments, indicating that its activity is not suppressed by tension-induced conformational changes in its kinetochore substrates. Several other mechanisms could explain the tension dependence of Aurora B, including the possibility that tension directly across Aurora B or the CPC could inactivate the kinase[54], or that the phosphatase, rather than the kinase, could be regulated by tension. Immunofluorescence has revealed a secondary pool of active Aurora B, close to the outer kinetochore and distinct from the inner-centromeric pool[55], leading to the attractive possibility that this secondary pool of Aurora B might localize specifically to kinetochores lacking tension and be depleted only upon the establishment of tension[56]. The flow assay we developed here can be used in the future to test these other models of Aurora B-based error correction, to help uncover how this important kinase senses tension and ultimately ensures the accuracy of chromosome segregation.

Online Methods

Protein preparation

The AurB* gene was created in several steps. First, the non-expressed linker between the *SLI15* and *IPL1* genes was removed on two polycistronic vectors expressing the four members of the CPC: pDD2396 (wild-type kinase) and pDD2399 (kinase-dead)[57]. A TEV cleavage site was added between the 6xHis tag and the *IPL1* gene in each plasmid and then the entire *SLI15-IPL1-*

TEV-6xHis genes from these constructs were amplified via PCR with BamHI and XhoI sites on the 5' and 3' ends, respectively, and inserted them into cut pET21b vectors (EMD Biosciences). Each kinase was then expressed as a single polypeptide with a T7 tag on its N-terminus and a 6xHis tag on its C-terminus (plasmids pSB2540 and pSB2894 for wild-type and kinase-dead, respectively). For protein preparation, each plasmid was co-transformed into the Tuner pLys BL21 (DE3) *E. coli* strain (Novagen) with a plasmid that encodes lambda phosphatase[58]. A single transformant was grown to OD 0.9 and expression of both proteins induced with 500 μM IPTG. Protein was expressed for four hours at 30 °C before harvesting. Cells were resuspended in prep buffer (50 mM Tris-HCl pH 7.4, 300 mM KCl, 5 mM $MgCl_2$, 5 mM ATP, 1 mM DTT, 20 mM imidazole, 10% glycerol) supplemented with 1% Triton X-100, 1 μL Turbo nuclease (Accelagen) and one tablet of Complete EDTA-free protease inhibitor (Roche) [57] and then lysed via incubation with 0.5 mg/mL lysozyme followed by sonication. Lysate was cleared by centrifugation and then applied to a column of Ni-NTA resin (Qiagen). Column was washed with 10 column volumes (CVs) of prep buffer and then protein-bound resin was resuspended in 3 CVs of prep buffer. DTT was added to 1 mM and 3 mg of TEV protease was added for three hours of room temperature incubation. TEV protease was expressed and purified in house[59]. The resin slurry was re-applied to the empty column and the flow-through was collected along with the flow-through from one wash. This was concentrated and applied to a Superdex 200 FPLC column with storage buffer (50 mM Tris-HCl pH 7.4, 300 mM NaCl, 10% glycerol, 50 mM arginine, 50 mM glutamate). Fractions were analyzed by SDS-PAGE and those from the main peak that eluted at 72 mL were pooled and concentrated.

Kinetochores were purified from budding yeast as previously described[41]. Kinetochore strains have a Dsn1 protein with 6xHis and 3xFlag tags on its C-terminus. Wild-type kinetochores

were purified from strain SBY8253; Mps1-1 kinetochores were from SBY8726; Ndc80-7A kinetochores were from SBY8522. Yeast strains were grown asynchronously to OD 4 at room temperature, harvested, washed, and resuspended in Buffer H (25 mM HEPES pH 8.0, 150 mM KCl, 2 mM $MgCl_2$, 0.1 mM EDTA pH 8.0, 0.1% NP-40, 15% glycerol) supplemented with protease inhibitors, phosphatase inhibitors and 2 mM DTT. SBY8726 for the purification of Mps1-1 was shifted to 37 °C for the last two hours of growth. After harvest, yeast drops were frozen in liquid nitrogen and then lysed using a Freezer Mill (SPEX). Lysate was clarified via ultracentrifugation at 24,000 rpm for 90 minutes and protein-containing layer was extracted with a syringe. Extract was incubated with magnetic Dynabeads previously conjugated to anti-flag antibodies for two hours at 4°C and then washed five times in Buffer H. For optical trapping assays, protein was eluted by incubating with 0.83 mg/mL 3xFlag peptide and quantified by comparing the Dsn1 silver-stained band to BSA standards. For enzyme assays, kinetochores were washed but then left attached to beads.

Dam1 complex was purified via a flag-tagged Dad1 protein[47] using a similar protocol. Dam1 complex was purified from strain SBY12464 identically to kinetochores except the initial immunoprecipitate was first washed three times with a Buffer H with 400 mM KCl before being washed twice in regular Buffer H. The complex was eluted by incubating with 0.83 mg/mL 3xFlag peptide and quantified by comparing the Spc34 silver-stained band to BSA standards.

Taxol-stabilized microtubules were grown by incubation of a mix of unlabeled and Alexa 647-labeled purified bovine tubulin in 1xBRB80 with 4.4% DMSO, 3.2 mM $MgCl_2$, and 0.8 mM GTP at 37°C for 30 minutes. Microtubules and unpolymerized tubulin were separated by ultracentrifugation and sedimented material was resuspended in 1xBRB80 with 10 μM taxol. Stabilized microtubules were used up to three days after polymerization.

Enzyme assays

For the radioactive kinase assays shown in Fig. 1, kinetochores were purified and immobilized on magnetic beads and then incubated with AurB*, AurB*-KD, or buffer with 0.2 μM hot (^{32}P-γ-labeled) and 200 μM cold ATP for the indicated periods of time at room temperature. Experiments were quenched in sample buffer and separated by SDS-PAGE before being silver stained. Gel was dried and exposed to a storage phosphor screen for longer than 48 hours for detection of incorporated ^{32}P.

For the microtubule binding assays shown in Figs. 2 and S1, Wild-type or Ndc80-7A kinetochores were purified and immobilized on beads, incubated with 80 nM purified Dam1 complex for 15 minutes, washed, then incubated in 1xBRB80 with 500 μM ATP, 1.8 mg/mL κ-casein, 20 μM taxol, and taxol-stabilized fluorescently-labeled microtubules for 5 minutes. At t=0, an aliquot was removed, washed with 1xBRB80 with 20 μM taxol and 0.01% Tween-20, and quenched with sample buffer. Buffer or 1 μM AurB* was added to each experiment after initial aliquot removal and further aliquots were removed, washed and quenched at the indicated times. The entire experiment occurred at room temperature. Samples were eluted from beads via boiling, separated by SDS-PAGE, and then analyzed via Western blot and fluorescence scan.

Immunoblotting

For Western blots, proteins were transferred from SDS-PAGE gels onto 0.22 μM cellulose paper, blocked at room temperature with 4% milk in PBST, and incubated overnight at 4°C in primary antibody. Antibody origins and dilutions in PBST were as follows: Ndc80 N-terminus: Desai lab 1:10,000; Flag: Sigma M2 1:3000; Myc: Covance 9E10 1:10,000; tubulin: EMD

Millipore YL1/2 1:1000. Blots were then washed again with PBST and incubated with secondary antibody at room temperature. Secondary antibodies were α-mouse, α-rabbit, or α-rat horseradish peroxidase-conjugated, from GE Healthcare, and used at 1:1000 dilution in 4% milk in PBST. Blots were then washed again with PBST and ECL substrate from Thermo Scientific used to visualize the proteins.

Optical trapping

The optical trapping was performed as described previously[30,41], with some modification to the reaction buffer and with the addition of flow. Bead conjugation and microtubule seed preparation were as previously described. Polystyrene beads conjugated to anti-His antibodies were incubated with Mps1-1 kinetochores at a concentration of 9.0 nM Dsn1 for 1 hour at 4 °C. This concentration is 50% higher than in our previous force-clamping experiments and potentially resulted in multiple kinetochore particles binding to a single microtubule. Reaction chambers were constructed on glass slides using sodium hydroxide- and ethanol-cleaned coverslips for an approximately 14 μL volume chamber. Coverslip-anchored microtubules were grown via successive introduction of: biotinylated bovine serum albumin, BRB80, avidin DN, BRB80, GMPCPP-stabilized microtubule seeds, GTP- and κ-casein-containing BRB80, and then a final reaction buffer consisting of BRB80, 0.3 mg/mL κ-casein, 1 mM GTP, 2% pluronic, 0.8 mM DTT, 48 mM glucose, 1.6 mg/mL glucose oxidate, 0.3 mg/mL catalase, 3 nM purified Dam1 complex, 400 μM ATP, bead-bound kinetochores, and 2.6 mg/mL unpolymerized tubulin. This is similar to previous versions of the optical trap assay except with lower casein and with the addition of pluronic and ATP. Additionally, the trap stiffness was set to the lowest possible level, 0.045 pN/nm, in order to minimize extra material becoming caught in the trap. During an experiment,

the laser was used to manipulate one bead to bind to the side of a dynamic microtubule tip. Then the bead was clamped at 5 pN of force and dragged to the tip. After 90 seconds of tracking with the tip at 5 pN, the force was either dropped to 1 pN, left at 5 pN, or elevated to 8 pN. Continued tip tracking was confirmed at the new force (~20 seconds) and then 20 μL of kinase-containing flow buffer was introduced via capillary action. Flow buffer contained BRB80, 0.3 mg/mL κ-casein, 1 mM GTP, 2% pluronic, 0.8 mM DTT, 48 mM glucose, 1.6 mg/mL gluocose oxidate, 0.3 mg/mL catalase, 500 μM ATP, 2.4 mg/mL tubulin and 8.6 μM AurB* or AurB*-KD. Flow in the chamber occurred immediately and was observed in the DIC view on the microscope. Events were observed without interference until either a rupture of the attachment occurred, or the event was ended by a second bead falling into the trap or by the bead tracking permanently back to the microtubule seed. Detachment rates were calculated by dividing the total number of detachments observed under a given condition by the total attachment time recorded. Uncertainties were estimated by dividing the detachment rate by the square root of the number of detachments. Kaplan-Meier analyses, including error analysis, were performed by Prism (GraphPad). The rupture force assay for Fig. S3a was performed under conditions identical to those previously described[53].

Data availability

The authors declare that the main data supporting the findings of this study are available within the article and its Supplementary Information files. Extra data are available from the corresponding author upon request.

Acknowledgements

We thank Arshad Desai for antibodies. We also thank Trisha Davis, Hironori Funabiki and members of the S.B. and C.L.A. labs for critical reading of the manuscript. A.K.D. is a Postdoctoral Fellow of the American Cancer Society. This work was supported by that fellowship, Packard Fellowship 2006-30521 (to C.L.A.), and NIH grants R01GM079373 (to C.L.A) and R01GM064386 (to S.B.). S.B. is also an investigator of the Howard Hughes Medical Institute.

Author Contributions

A.K.D. conceptually designed and performed experiments, analyzed the data, and wrote the manuscript; C.L.A. and S.B. conceptually designed experiments, analyzed the data, and wrote the manuscript with A.K.D.

Competing Interests

The authors declare no competing interests.

References

1 Cheeseman, I. M. & Desai, A. Molecular architecture of the kinetochore-microtubule interface. *Nature reviews. Molecular cell biology* **9**, 33-46, doi:10.1038/nrm2310 (2008).

2 Santaguida, S. & Musacchio, A. The life and miracles of kinetochores. *The EMBO journal* **28**, 2511-2531, doi:10.1038/emboj.2009.173 (2009).

3 Nicklas, R. B. & Koch, C. A. Chromosome micromanipulation. 3. Spindle fiber tension and the reorientation of mal-oriented chromosomes. *The Journal of cell biology* **43**, 40-50 (1969).

4 Nicklas, R. B. & Ward, S. C. Elements of error correction in mitosis: microtubule capture, release, and tension. *The Journal of cell biology* **126**, 1241-1253 (1994).

5 Biggins, S. *et al.* The conserved protein kinase Ipl1 regulates microtubule binding to kinetochores in budding yeast. *Genes Dev* **13**, 532-544 (1999).

6 Tanaka, T. U. *et al.* Evidence that the Ipl1-Sli15 (Aurora kinase-INCENP) complex promotes chromosome bi-orientation by altering kinetochore-spindle pole connections. *Cell* **108**, 317-329 (2002).

7 Lampson, M. A., Renduchitala, K., Khodjakov, A. & Kapoor, T. M. Correcting improper chromosome-spindle attachments during cell division. *Nat Cell Biol* **6**, 232-237, doi:10.1038/ncb1102 (2004).

8 Cheeseman, I. M., Chappie, J. S., Wilson-Kubalek, E. M. & Desai, A. The conserved KMN network constitutes the core microtubule-binding site of the kinetochore. *Cell* **127**, 983-997, doi:10.1016/j.cell.2006.09.039 (2006).

9 Cimini, D., Wan, X., Hirel, C. B. & Salmon, E. D. Aurora kinase promotes turnover of kinetochore microtubules to reduce chromosome segregation errors. *Current biology : CB* **16**, 1711-1718, doi:10.1016/j.cub.2006.07.022 (2006).

10 DeLuca, J. G. *et al.* Kinetochore microtubule dynamics and attachment stability are regulated by Hec1. *Cell* **127**, 969-982, doi:10.1016/j.cell.2006.09.047 (2006).

11 Kelly, A. E. & Funabiki, H. Correcting aberrant kinetochore microtubule attachments: an Aurora B-centric view. *Current opinion in cell biology* **21**, 51-58, doi:10.1016/j.ceb.2009.01.004 (2009).

12 Liu, D., Vader, G., Vromans, M. J., Lampson, M. A. & Lens, S. M. Sensing chromosome bi-orientation by spatial separation of aurora B kinase from kinetochore substrates. *Science (New York, N.Y.)* **323**, 1350-1353, doi:10.1126/science.1167000 (2009).

13 Welburn, J. P. *et al.* Aurora B phosphorylates spatially distinct targets to differentially regulate the kinetochore-microtubule interface. *Molecular cell* **38**, 383-392, doi:10.1016/j.molcel.2010.02.034 (2010).

14 Yue, Z. *et al.* Deconstructing Survivin: comprehensive genetic analysis of Survivin function by conditional knockout in a vertebrate cell line. *The Journal of cell biology* **183**, 279-296, doi:10.1083/jcb.200806118 (2008).

15 Campbell, C. S. & Desai, A. Tension sensing by Aurora B kinase is independent of survivin-based centromere localization. *Nature* **497**, 118-121, doi:10.1038/nature12057 (2013).

16 Hengeveld, R. C. C., Vromans, M. J. M., Vleugel, M., Hadders, M. A. & Lens, S. M. A. Inner centromere localization of the CPC maintains centromere cohesion and allows mitotic checkpoint silencing. *Nature communications* **8**, 15542, doi:10.1038/ncomms15542 (2017).

17 Katayama, H., Brinkley, W. R. & Sen, S. The Aurora kinases: role in cell transformation and tumorigenesis. *Cancer metastasis reviews* **22**, 451-464 (2003).

18 Katayama, H. *et al.* Mitotic kinase expression and colorectal cancer progression. *Journal of the National Cancer Institute* **91**, 1160-1162 (1999).

19 Tatsuka, M. *et al.* Multinuclearity and increased ploidy caused by overexpression of the aurora- and Ipl1-like midbody-associated protein mitotic kinase in human cancer cells. *Cancer research* **58**, 4811-4816 (1998).

20 Lens, S. M. *et al.* Uncoupling the central spindle-associated function of the chromosomal passenger complex from its role at centromeres. *Molecular biology of the cell* **17**, 1897-1909, doi:10.1091/mbc.e05-08-0727 (2006).

21 Ruchaud, S., Carmena, M. & Earnshaw, W. C. Chromosomal passengers: conducting cell division. *Nature reviews. Molecular cell biology* **8**, 798-812, doi:10.1038/nrm2257 (2007).

22 Adams, R. R. *et al.* INCENP binds the Aurora-related kinase AIRK2 and is required to target it to chromosomes, the central spindle and cleavage furrow. *Current biology : CB* **10**, 1075-1078 (2000).

23 Bishop, J. D. & Schumacher, J. M. Phosphorylation of the carboxyl terminus of inner centromere protein (INCENP) by the Aurora B Kinase stimulates Aurora B kinase activity. *The Journal of biological chemistry* **277**, 27577-27580, doi:10.1074/jbc.C200307200 (2002).

24 Bolton, M. A. *et al.* Aurora B kinase exists in a complex with survivin and INCENP and its kinase activity is stimulated by survivin binding and phosphorylation. *Molecular biology of the cell* **13**, 3064-3077, doi:10.1091/mbc.E02-02-0092 (2002).

25 Honda, R., Korner, R. & Nigg, E. A. Exploring the functional interactions between Aurora B, INCENP, and survivin in mitosis. *Molecular biology of the cell* **14**, 3325-3341, doi:10.1091/mbc.E02-11-0769 (2003).

26 Kaitna, S., Mendoza, M., Jantsch-Plunger, V. & Glotzer, M. Incenp and an aurora-like kinase form a complex essential for chromosome segregation and efficient completion of cytokinesis. *Current biology : CB* **10**, 1172-1181 (2000).

27 Kang, J. *et al.* Functional cooperation of Dam1, Ipl1, and the inner centromere protein (INCENP)-related protein Sli15 during chromosome segregation. *The Journal of cell biology* **155**, 763-774, doi:10.1083/jcb.200105029 (2001).

28 Wang, E., Ballister, E. R. & Lampson, M. A. Aurora B dynamics at centromeres create a diffusion-based phosphorylation gradient. *The Journal of cell biology* **194**, 539-549, doi:10.1083/jcb.201103044 (2011).

29 Umbreit, N. T. *et al.* The Ndc80 kinetochore complex directly modulates microtubule dynamics. *Proceedings of the National Academy of Sciences of the United States of America* **109**, 16113-16118, doi:10.1073/pnas.1209615109 (2012).

30 Sarangapani, K. K., Akiyoshi, B., Duggan, N. M., Biggins, S. & Asbury, C. L. Phosphoregulation promotes release of kinetochores from dynamic microtubules via multiple mechanisms. *Proceedings of the National Academy of Sciences of the United States of America* **110**, 7282-7287, doi:10.1073/pnas.1220700110 (2013).

31 Smith, C. A., McAinsh, A. D. & Burroughs, N. J. Human kinetochores are swivel joints that mediate microtubule attachments. *eLife* **5**, doi:10.7554/eLife.16159 (2016).

32 Wan, X. *et al.* Protein architecture of the human kinetochore microtubule attachment site. *Cell* **137**, 672-684, doi:10.1016/j.cell.2009.03.035 (2009).

33 Tien, J. F. *et al.* Kinetochore biorientation in *Saccharomyces cerevisiae* requires a tightly folded conformation of the Ndc80 complex. *Genetics* **198**, 1483-1493, doi:10.1534/genetics.114.167775 (2014).

34 Joglekar, A. P., Bloom, K. & Salmon, E. D. In vivo protein architecture of the eukaryotic kinetochore with nanometer scale accuracy. *Curr Biol* **19**, 694-699, doi:10.1016/j.cub.2009.02.056 (2009).

35 Campbell, I. D. & Humphries, M. J. Integrin structure, activation, and interactions. *Cold Spring Harbor perspectives in biology* **3**, doi:10.1101/cshperspect.a004994 (2011).

36 Ranade, S. S., Syeda, R. & Patapoutian, A. Mechanically Activated Ion Channels. *Neuron* **87**, 1162-1179, doi:10.1016/j.neuron.2015.08.032 (2015).

37 Liu, D. *et al.* Regulated targeting of protein phosphatase 1 to the outer kinetochore by KNL1 opposes Aurora B kinase. *The Journal of cell biology* **188**, 809-820, doi:10.1083/jcb.201001006 (2010).

38 Foley, E. A., Maldonado, M. & Kapoor, T. M. Formation of stable attachments between kinetochores and microtubules depends on the B56-PP2A phosphatase. *Nature cell biology* **13**, 1265-1271, doi:10.1038/ncb2327 (2011).

39 Suijkerbuijk, S. J., Vleugel, M., Teixeira, A. & Kops, G. J. Integration of kinase and phosphatase activities by BUBR1 ensures formation of stable kinetochore-microtubule attachments. *Developmental cell* **23**, 745-755, doi:10.1016/j.devcel.2012.09.005 (2012).

40 Kruse, T. *et al.* Direct binding between BubR1 and B56-PP2A phosphatase complexes regulate mitotic progression. *Journal of cell science* **126**, 1086-1092, doi:10.1242/jcs.122481 (2013).

41 Akiyoshi, B. *et al.* Tension directly stabilizes reconstituted kinetochore-microtubule attachments. *Nature* **468**, 576-579, doi:10.1038/nature09594 (2010).

42 London, N., Ceto, S., Ranish, J. A. & Biggins, S. Phosphoregulation of Spc105 by Mps1 and PP1 regulates Bub1 localization to kinetochores. *Current biology : CB* **22**, 900-906, doi:10.1016/j.cub.2012.03.052 (2012).

43 Meyer, R. E. *et al.* Mps1 and Ipl1/Aurora B act sequentially to correctly orient chromosomes on the meiotic spindle of budding yeast. *Science (New York, N.Y.)* **339**, 1071-1074, doi:10.1126/science.1232518 (2013).

44 Akiyoshi, B., Nelson, C. R., Ranish, J. A. & Biggins, S. Analysis of Ipl1-mediated phosphorylation of the Ndc80 kinetochore protein in *Saccharomyces cerevisiae*. *Genetics* **183**, 1591-1595, doi:10.1534/genetics.109.109041 (2009).

45 Akiyoshi, B., Nelson, C. R. & Biggins, S. The aurora B kinase promotes inner and outer kinetochore interactions in budding yeast. *Genetics* **194**, 785-789, doi:10.1534/genetics.113.150839 (2013).

46 Hauf, S. *et al.* The small molecule Hesperadin reveals a role for Aurora B in correcting kinetochore-microtubule attachment and in maintaining the spindle assembly checkpoint. *The Journal of cell biology* **161**, 281-294, doi:10.1083/jcb.200208092 (2003).

47 Cheeseman, I. M. *et al.* Implication of a novel multiprotein Dam1p complex in outer kinetochore function. *The Journal of cell biology* **155**, 1137-1145, doi:10.1083/jcb.200109063 (2001).

48 Ciferri, C. *et al.* Implications for kinetochore-microtubule attachment from the structure of an engineered Ndc80 complex. *Cell* **133**, 427-439, doi:10.1016/j.cell.2008.03.020 (2008).

49 Gestaut, D. R. *et al.* Phosphoregulation and depolymerization-driven movement of the Dam1 complex do not require ring formation. *Nature cell biology* **10**, 407-414, doi:10.1038/ncb1702 (2008).

50 Kalantzaki, M. *et al.* Kinetochore-microtubule error correction is driven by differentially regulated interaction modes. *Nat Cell Biol* **17**, 421-433, doi:10.1038/ncb3128 (2015).

51 Umbreit, N. T. *et al.* Kinetochores require oligomerization of Dam1 complex to maintain microtubule attachments against tension and promote biorientation. *Nature communications* **5**, 4951, doi:10.1038/ncomms5951 (2014).

52 Sarangapani, K. K. *et al.* Sister kinetochores are mechanically fused during meiosis I in yeast. *Science (New York, N.Y.)* **346**, 248-251, doi:10.1126/science.1256729 (2014).

53 Miller, M. P., Asbury, C. L. & Biggins, S. A TOG Protein Confers Tension Sensitivity to Kinetochore-Microtubule Attachments. *Cell* **165**, 1428-1439, doi:10.1016/j.cell.2016.04.030 (2016).

54 Sandall, S. *et al.* A Bir1-Sli15 complex connects centromeres to microtubules and is required to sense kinetochore tension. *Cell* **127**, 1179-1191, doi:10.1016/j.cell.2006.09.049 (2006).

55 DeLuca, K. F., Lens, S. M. & DeLuca, J. G. Temporal changes in Hec1 phosphorylation control kinetochore-microtubule attachment stability during mitosis. *Journal of cell science* **124**, 622-634, doi:10.1242/jcs.072629 (2011).

56 Caldas, G. V., DeLuca, K. F. & DeLuca, J. G. KNL1 facilitates phosphorylation of outer kinetochore proteins by promoting Aurora B kinase activity. *The Journal of cell biology* **203**, 957-969, doi:10.1083/jcb.201306054 (2013).

57 Cormier, A., Drubin, D. G. & Barnes, G. Phosphorylation regulates kinase and microtubule binding activities of the budding yeast chromosomal passenger complex in vitro. *The Journal of biological chemistry* **288**, 23203-23211, doi:10.1074/jbc.M113.491480 (2013).

58 Brading, R. L., Abbott, W. M., Green, I., Davies, A. & McCall, E. J. Co-expression of protein phosphatases in insect cells affects phosphorylation status and expression levels of

proteins. *Protein expression and purification* **83**, 217-225, doi:10.1016/j.pep.2012.04.006 (2012).

59 Tropea, J. E., Cherry, S. & Waugh, D. S. Expression and purification of soluble His(6)-tagged TEV protease. *Methods in molecular biology (Clifton, N.J.)* **498**, 297-307, doi:10.1007/978-1-59745-196-3_19 (2009).

Figure Legends

Fig. 1 | An Aurora B kinase phosphorylates kinetochores. a AurB* was created by fusing the C-terminal activation box of INCENP^{Sli15} to Aurora B^{Ipl1}. **b** Schematic for the experiments shown in (**c**)-(**e**). **c** Mps1-1 kinetochores (purified from SBY8726) were phosphorylated by either 0.2 μM AurB* or 0.2 μM AurB*-KD and ^{32}P-γ-labeled ATP and then visualized by silver stain and autoradiography. The first two lanes show AurB* or AurB*-KD alone with no kinetochores after 5 minutes of incubation, the next five lanes show a time course of kinetochores incubated with AurB*, and each of the last two lanes show kinetochores incubated with either no kinase or AurB*-KD for 3.5 minutes. The bands of relevant Aurora B substrates are labeled. Positions of protein standards are shown on the left in kDa. **d** Quantification of Ndc80 incorporation of ^{32}P in (**c**). Red points (AurB*) are from the time course, the blue point (ATP only) is from the second to last lane, and the grey point (AurB*-KD) is from the last lane. Units are arbitrary and relative. **e** Wild type (SBY8253) or Ndc80-7A (SBY8522) kinetochores (KT) were incubated with either buffer or 1 μM AurB* and ^{32}P-γ-labeled ATP for 3 minutes. A decrease in phosphorylation in the Ndc80 band when comparing lanes 2 and 4 show that AurB* is phosphorylating Ndc80 on these seven known sites.

Fig. 2 | Aurora B phosphorylation is sufficient for kinetochores' release of microtubules. a Schematic for the experiment shown in (**b**). **b** Purified wild-type (WT) (SBY8253) or Ndc80-7A (SBY8522) kinetochores were bound to purified Dam1 complex (Dam1c; SBY12464) and then to taxol-stabilized fluorescently-labeled microtubules in the presence of ATP. Buffer or 1 μM AurB* was then added and components retained after a wash were separated via SDS-PAGE and visualized by Western blot and fluorescence scan. *P*-Ndc80: phosphorylated Ndc80. **c** Quantification of bound microtubules (lowest row in (**b**)) presented as the average of three independent experiments; error bars represent standard deviations. Values were normalized to microtubules bound at t=0. P values between the t=20 timepoints using an unpaired t-test are as follows: 0.0054 (WT+buffer/WT+AurB*), 0.16 (WT+buffer/7A+AurB*), 0.033 (WT+AurB*/7A+AurB*).

Fig. 3 | A flow assay introduces Aurora B to a kinetochore-microtubule attachment under tension. a Schematic of the optical trap flow assay. Tension across kinetochore-microtubule

attachments is proportional to the displacement of the bead from the center of the laser trap. **b, c** Traces of optical trap data for two individual events. Gray points show the force applied and green points show the same data after smoothing. Blue traces show the relative position of the stage over time. Kinase introduction occurred at time 0 seconds; blue shading indicates data before kinase introduction. (**b**) shows an event that ended when a second bead became caught in the laser trap and corresponds to Movie 1. (**c**) shows an event that ended in a detachment and corresponds to Movie 2. The yellow ball indicates when detachment occurred.

Fig. 4 | Aurora B phosphorylation is sufficient to release kinetochores from the tips of dynamic microtubules. a Each individual event, corresponding to one bead, graphed as a bar whose length corresponds to its total time. Events that ended in detachment are marked with yellow balls. Events that were interrupted are unmarked. Asterisks indicate the events shown in Figs. 3b-c. **b** Kaplan-Meier survival analysis for flow with AurB*-KD or AurB*. AurB*-KD was flowed in at a final concentration of 5 μM and AurB* was flowed in at a final concentration of either 0.5 or 5 μM. Detachment rates at these concentrations of AurB* were indistinguishable from one another and were therefore pooled. Ticks indicate censored data points from interrupted events that did not end in detachment. Shaded errors show standard error. P = 0.014 using a log-rank test. **c** Detachment rates of kinetochores from microtubules held under 1.3 ± 0.6 pN or 1.1 ± 0.5 pN of force after flow with AurB*-KD or AurB*, respectively. Error bars represent uncertainty due to counting statistics (n = 26 beads and 7 detachments (AurB*-KD) and n = 28 beads and 18 detachments (AurB*)).

Fig. 5 | Tension does not suppress Aurora B-triggered detachment. a Detachment rates of kinetochores from microtubules at different forces with introduction of either 5 μM AurB* or 5 μM AurB*-KD. Some data from Fig. 4 are replotted here. **b** Kaplan-Meier survival analysis for flow with 5 μM AurB*-KD, 0.5 μM AurB*, or 5 μM AurB*. Ticks represent censored data points from interrupted events that did not end in detachment. Shaded errors show standard error. P values using a log-rank test are as follows: 0.040 (KD vs 0.5 μM AurB*), 0.0097 (0.5 μM vs 5 μM AurB*), <0.0001 (KD vs 5 μM AurB*). **c** Detachment rates of kinetochores from microtubules at different levels of AurB* kinase activity, where AurB*-KD is 0 μM AurB*. Kinetochores were held at 4.7 ± 0.6 pN (AurB*-KD), 4.8 ± 0.6 pN (0.5 μM AurB*), or 5.0 ± 0.2 pN (5 μM AurB*). Error bars represent uncertainty due to counting statistics (n = 20 events and 11 detachments (AurB*-KD), n = 4 events and 4 detachments (0.5 μM AurB*), or n = 12 events and 8 detachments (5 μM AurB*)).

Fig. S1 | Immunoblot of purified kinetochores from either wild-type (SBY8253) or Mps1-1 (SBY8726) kinetochores showing that Mps1-1 kinetochores lack co-purifying Dam1 complex.

Fig. S2 | a Schematic for microtubule binding experiment **b** Mps1-1 kinetochores (SBY8726) were incubated with microtubules and kinase for the times indicated in the presence or absence of ATP. Bound components were assayed by Western blot.

Fig. S3 | a Rupture force values for various kinetochores detaching from microtubules as determined using an optical force-ramp. Where indicated, exogenously purified Dam1 complex (Dam1c) and/or ATP were included in the trapping buffer. **b** Traces of optical trap data for an individual force-clamp event. Gray points show the force applied across the kinetochore-microtubule attachment and green points show the same data after smoothing. The blue trace shows the relative position of a single kinetochore-coupled bead as it tracks with the microtubule tip.

Fig. S4 | **a** Detachment rates for Mps1-1 kinetochores with Dam1 complex present, separated by concentration of kinase. The data at 1 pN and 5 pN are replotted from Figs. 4 and 5. For the data at 8 pN, n = 4 events and 2 detachments (AurB*-KD) or n = 3 events and 3 detachments (5 μM AurB*). **b** Detachment rates for wild-type kinetochores at high force. The assay was performed as diagramed in Fig. 3a, except with wild-type kinetochores and no addition of Dam1 complex. 5 μM of either AurB* or AurB*-KD was flowed in.

Fig. S5 | a and **b** Kinetochore detachment rates measured specifically during microtubule growth (**a**) and during microtubule shortening (**b**). Rates measured for this work, using Mps1-1 kinetochores with Dam1 complex and AurB*-KD flow, are shown in gray. Rates for wild-type kinetochores, from previous work [41,53], are shown in green.

Movie 1 | Differential interference contrast (DIC) view of an event during the flow assay that ends in an interruption, with a second bead falling into the trap; this event corresponds to the traces in Fig. 3b. Timer counts down until flow is introduced and then counts up. The second bead appears 2:23 after flow initiation.

Movie 2 | Differential interference contrast (DIC) view of an event during the flow assay that ends in a detachment; this event corresponds to the traces in Fig. 3c. Timer counts down until flow is introduced and then counts up. Detachment occurs at 5:12.

Figure 1

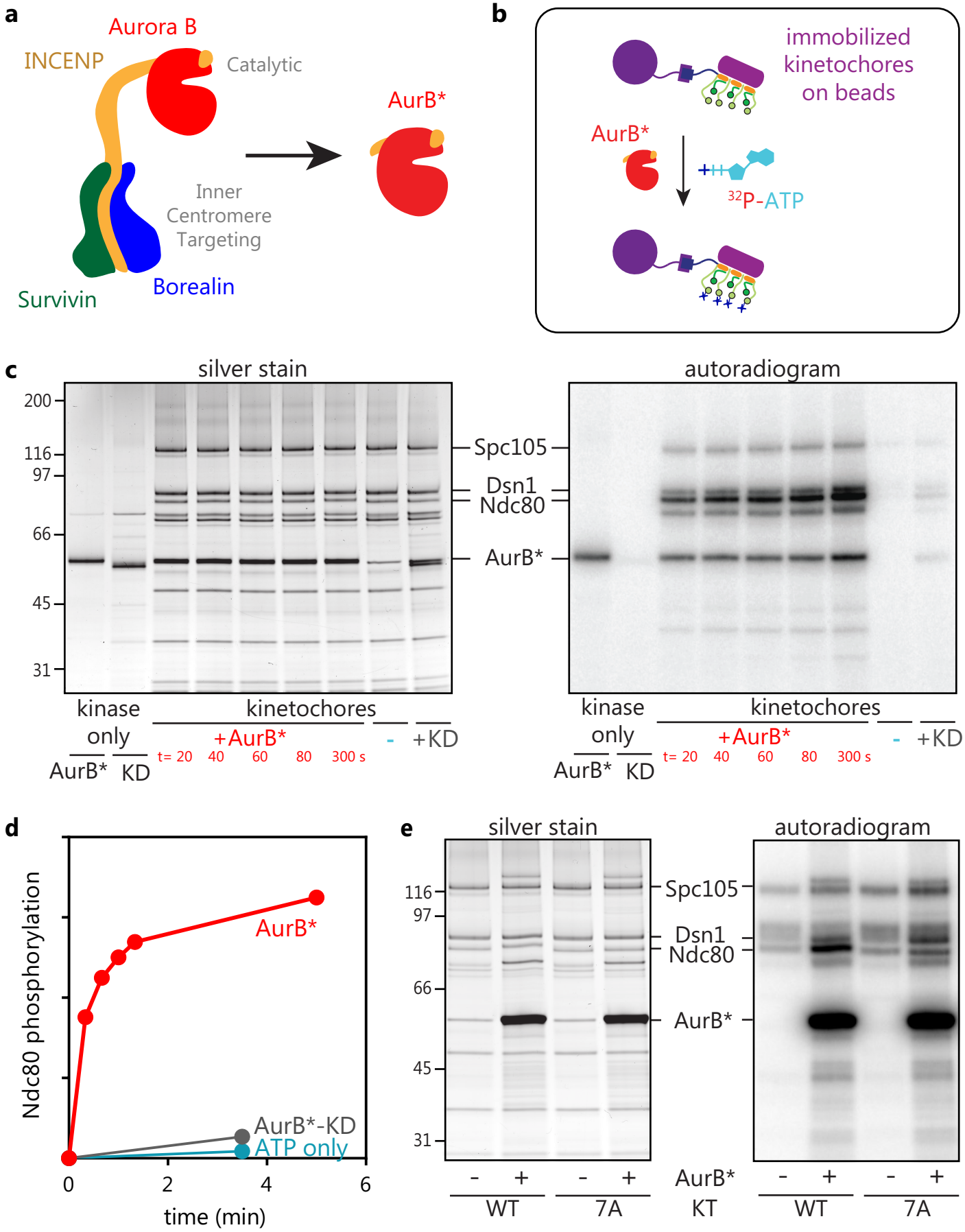
a
Aurora B
INCENP
Catalytic
AurB*
Inner
Centromere
Targeting
Survivin
Borealin
b
immobilized
kinetochores
on beads
AurB*
32P-ATP
c
silver stain
autoradiogram
200
116
97
66
45
31
Spc105
Dsn1
Ndc80
AurB*
kinase
only
kinetochores
+AurB*
-
+KD
AurB*
KD
t= 20
40
60
80
300 s
d
Ndc80 phosphorylation
AurB*
AurB*-KD
ATP only
0
2
4
6
time (min)
e
silver stain
autoradiogram
116
97
66
45
31
Spc105
Dsn1
Ndc80
AurB*
-
+
-
+
AurB*
-
+
-
+
WT
7A
KT
WT
7A

Fig. 1 | An Aurora B kinase phosphorylates kinetochores. a AurB* was created by fusing the C-terminal activation box of INCENP^{Sli15} to Aurora B^{Ipl1}. **b** Schematic for the experiments shown in (**c**)-(**e**). **c** Mps1-1 kinetochores (purified from SBY8726) were phosphorylated by either 0.2 μM AurB* or 0.2 μM AurB*-KD and ^{32}P-γ-labeled ATP and then visualized by silver stain and autoradiography. The first two lanes show AurB* or AurB*-KD alone with no kinetochores after 5 minutes of incubation, the next five lanes show a timecourse of kinetochores incubated with AurB*, and each of the last two lanes show kinetochores incubated with either no kinase or AurB*-KD for 3.5 minutes. The bands of relevant Aurora B substrates are labeled. Positions of protein standards are shown on the left in kDa. **d** Quantification of Ndc80 incorporation of ^{32}P in (**c**). Red points (AurB*) are from the timecourse, the blue point (ATP only) is from the second to last lane, and the grey point (AurB*-KD) is from the last lane. Units are arbitrary and relative. **e** Wild type (SBY8253) or Ndc80-7A (SBY8522) kinetochores (KT) were incubated with either buffer or 1 μM AurB* and ^{32}P-γ-labeled ATP for 3 minutes. A decrease in phosphorylation in the Ndc80 band when comparing lanes 2 and 4 show that AurB* is phosphorylating Ndc80 on these seven known sites.

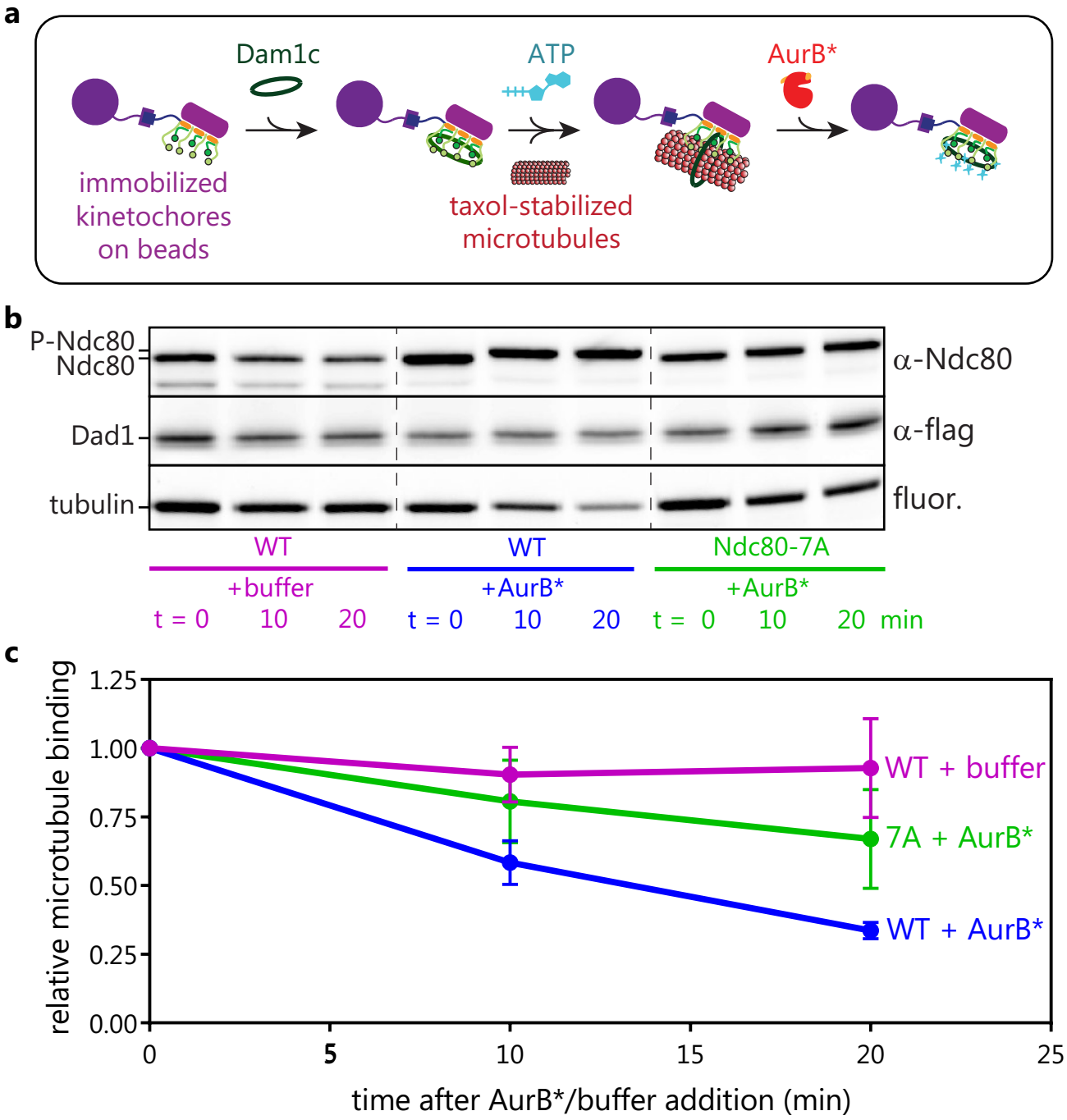

Fig. 2 | Aurora B phosphorylation is sufficient for kinetochores' release of microtubules. a Schematic for the experiment shown in (**b**). **b** Purified wild-type (WT) (SBY8253) or Ndc80-7A (SBY8522) kinetochores were bound to purified Dam1 complex (Dam1c; SBY12464) and then to taxol-stabilized fluorescently-labeled microtubules in the presence of ATP. Buffer or 1 μM AurB* was then added and components retained after a wash were separated via SDS-PAGE and visualized by Western blot and fluorescence scan. *P*-Ndc80: phosphorylated Ndc80. **c** Quantification of bound microtubules (lowest row in (**b**)) presented as the average of three independent experiments; error bars represent standard deviations. Values were normalized to microtubules bound at t=0. P values between the t=20 timepoints using an unpaired t-test are as follows: 0.0054 (WT+buffer/WT+AurB*), 0.16 (WT+buffer/7A+AurB*), 0.033 (WT+AurB*/7A+AurB*).

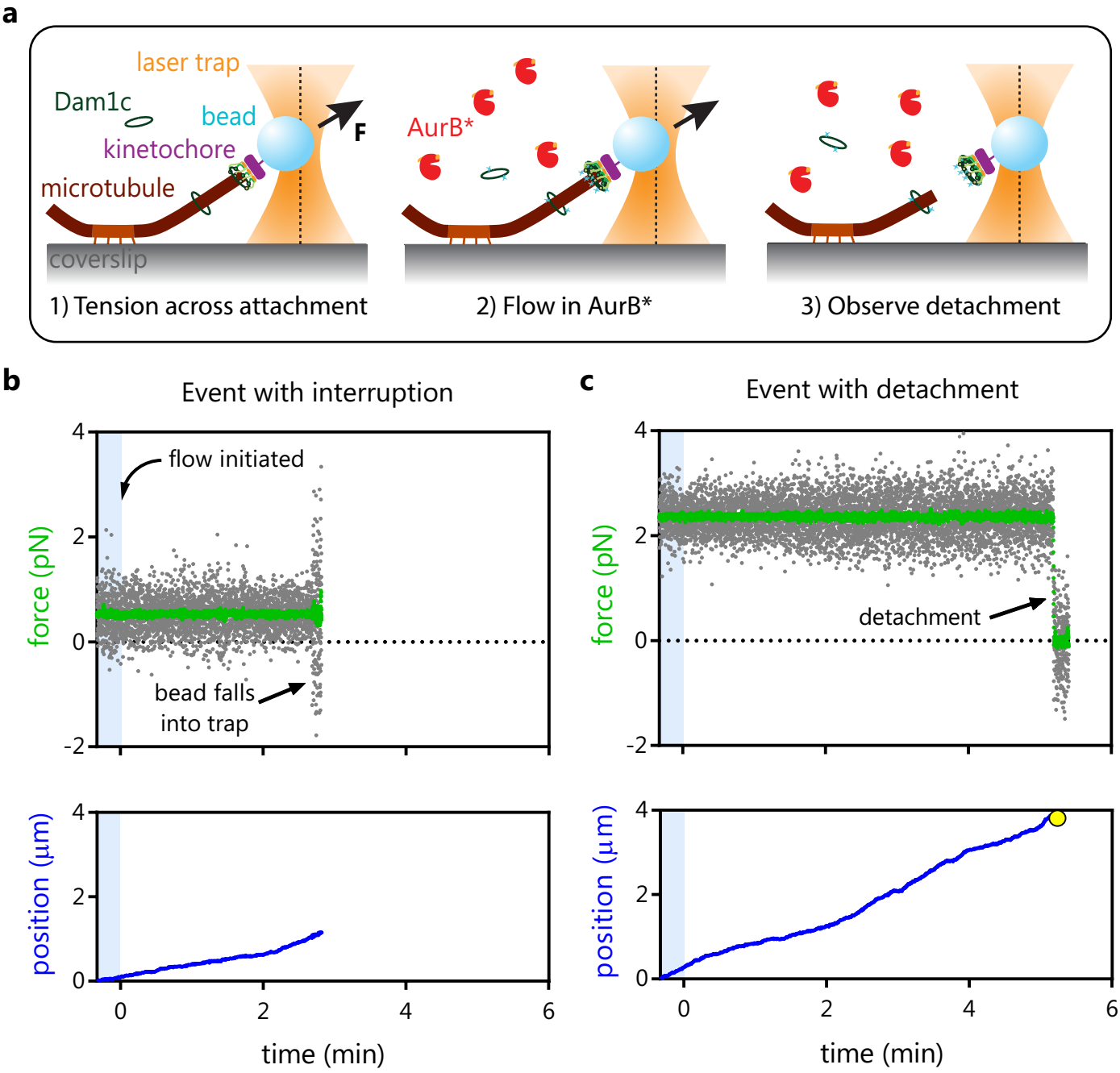

Fig. 3 | A flow assay introduces Aurora B to a kinetochore-microtubule attachment under tension. a Schematic of the optical trap flow assay. Tension across kinetochore-microtubule attachments is proportional to the displacement of the bead from the center of the laser trap. **b, c** Traces of optical trap data for two individual events. Gray points show the force applied and green points show the same data after smoothing. Blue traces show the relative position of the stage over time. Kinase introduction occurred at time 0 seconds; blue shading indicates data before kinase introduction. (**b**) shows an event that ended when a second bead became caught in the laser trap and corresponds to Movie 1. (**c**) shows an event that ended in a detachment and corresponds to Movie 2. The yellow ball indicates when detachment occurred.

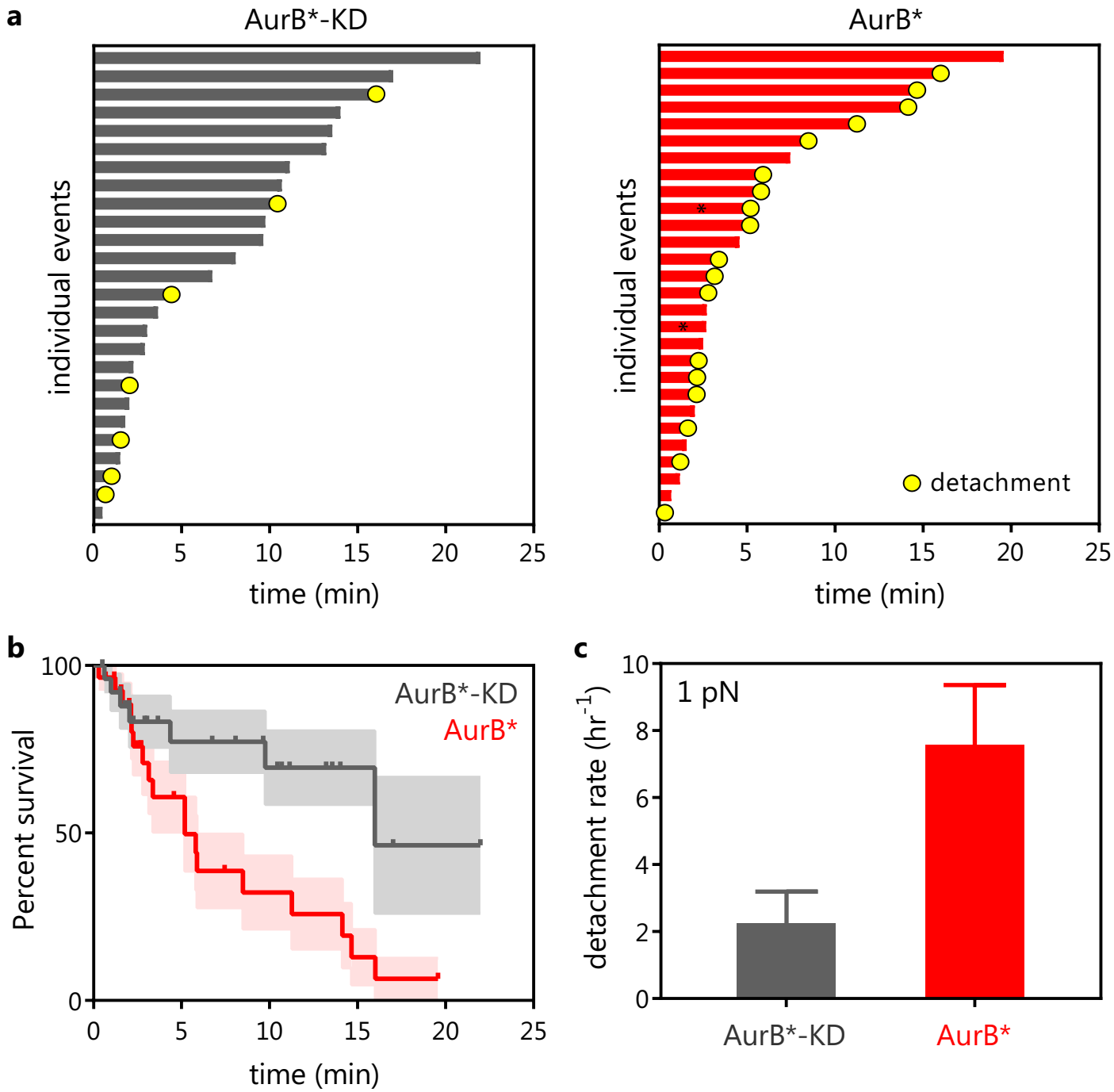

Fig. 4 | Aurora B phosphorylation is sufficient to release kinetochores from the tips of dynamic microtubules. **a** Each individual event, corresponding to one bead, graphed as a bar whose length corresponds to its total time. Events that ended in detachment are marked with yellow balls. Events that were interrupted are unmarked. Asterisks indicate the events shown in Figs. 3b-c. **b** Kaplan-Meier survival analysis for flow with AurB*-KD or AurB*. AurB*-KD was flowed in at a final concentration of 5 μM and AurB* was flowed in at a final concentration of either 0.5 or 5 μM. Detachment rates at these concentrations of AurB* were indistinguishable from one another and were therefore pooled. Ticks indicate censored data points from interrupted events that did not end in detachment. Shaded errors show standard error. P = 0.014 using a log-rank test. **c** Detachment rates of kinetochores from microtubules held under 1.3 ± 0.6 pN or 1.1 ± 0.5 pN of force after flow with AurB*-KD or AurB*, respectively. Error bars represent uncertainty due to counting statistics (n = 26 beads and 7 detachments (AurB*-KD) and n = 28 beads and 18 detachments (AurB*)).

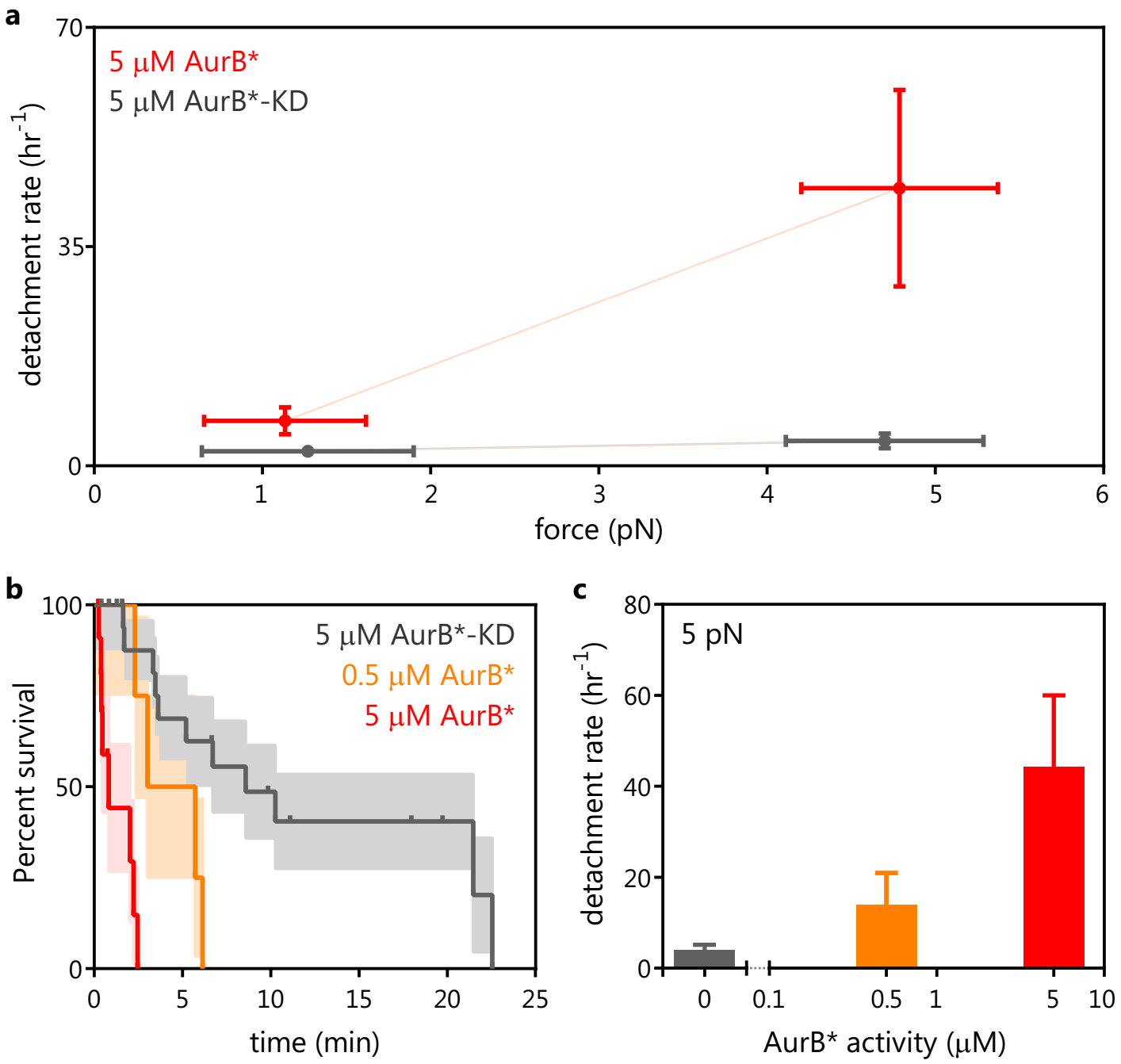

Fig. 5 | Tension does not suppress Aurora B-triggered detachment. a Detachment rates of kinetochores from microtubules at different forces with introduction of either 5 μM AurB* or 5 μM AurB*-KD. Some data from Fig. 4 are replotted here. **b** Kaplan-Meier survival analysis for flow with 5 μM AurB*-KD, 0.5 μM AurB*, or 5 μM AurB*. Ticks represent censored data points from interrupted events that did not end in detachment. Shaded errors show standard error. P values using a log-rank test are as follows: 0.040 (KD vs 0.5 μM AurB*), 0.0097 (0.5 μM vs 5 μM AurB*), <0.0001 (KD vs 5 μM AurB*). **c** Detachment rates of kinetochores from microtubules at different levels of AurB* kinase activity, where AurB*-KD is 0 μM AurB*. Kinetochores were held at 4.7 ± 0.6 pN (AurB*-KD), 4.8 ± 0.6 pN (0.5 μM AurB*), or 5.0 ± 0.2 pN (5 μM AurB*). Error bars represent uncertainty due to counting statistics (n = 20 events and 11 detachments (AurB*-KD), n = 4 events and 4 detachments (0.5 μM AurB*), or n = 12 events and 8 detachments (5 μM AurB*)).

Figure S1

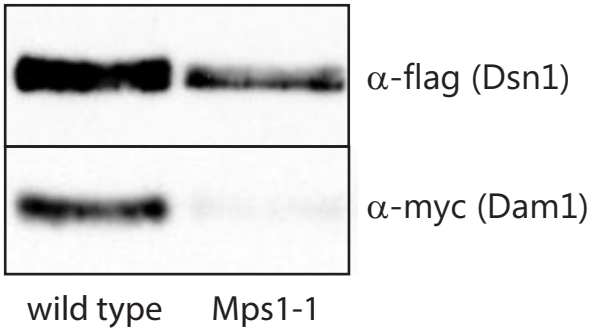

Fig. S1 | Immunoblot of purified kinetochores from either wild-type (SBY8253) or Mps1-1 (SBY8726) kinetochores showing that Mps1-1 kinetochores lack co-purifying Dam1 complex.

Figure S2

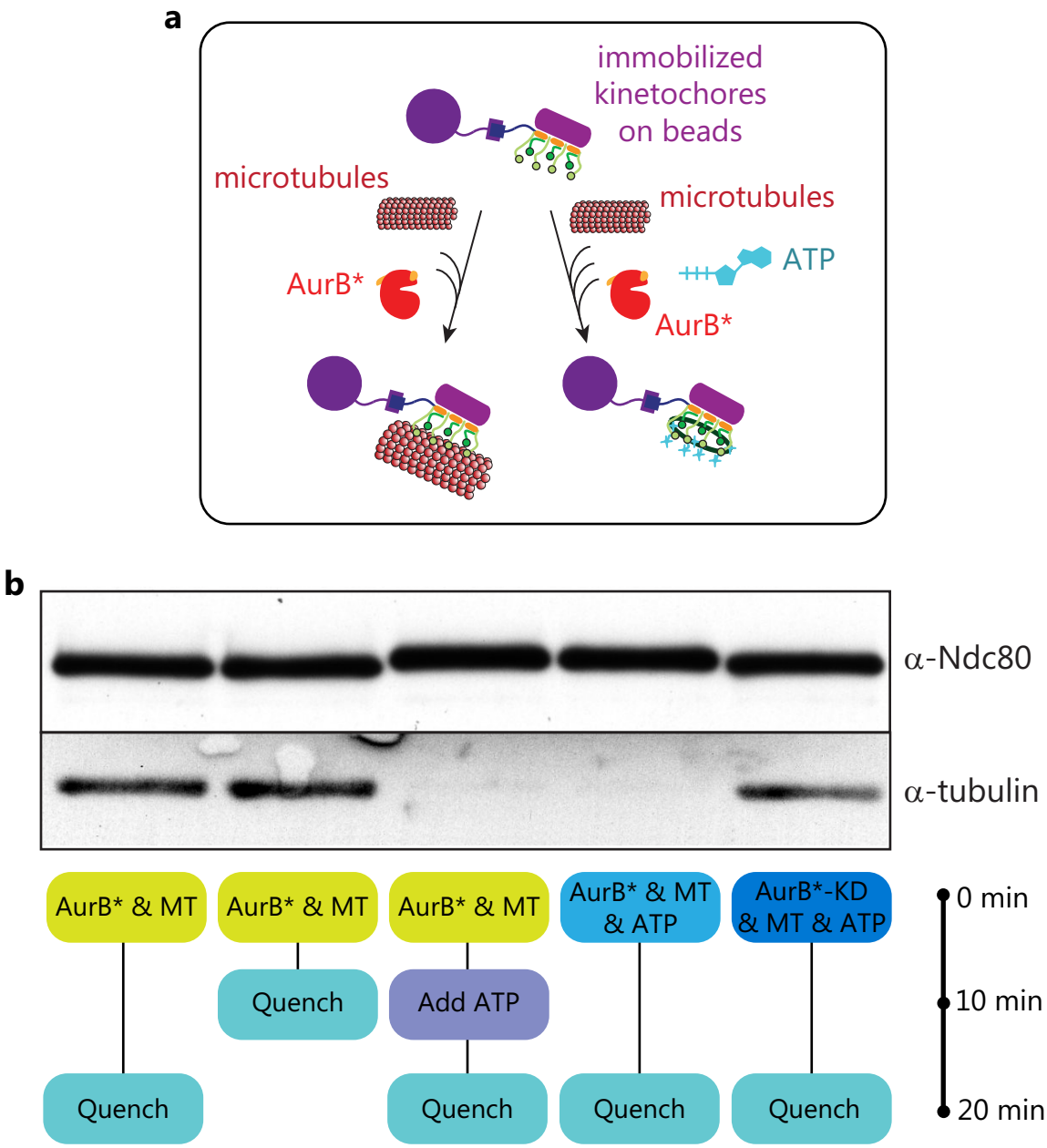

Fig. S2 | a Schematic for microtubule binding experiment **b** Mps1-1 kinetochores (SBY8726) were incubated with microtubules and kinase for the times indicated in the presence or absence of ATP. Bound components were assayed by Western blot.

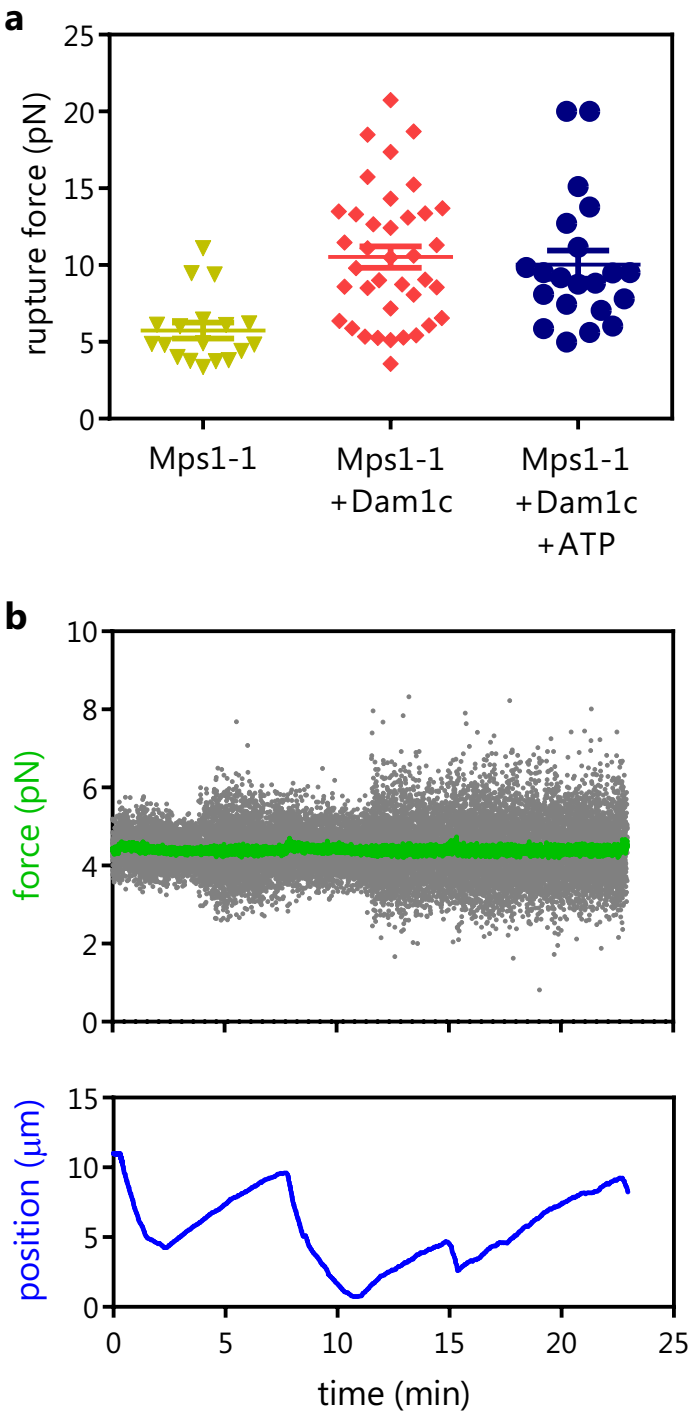

Fig. S3 | a Rupture force values for various kinetochores detaching from microtubules as determined using an optical force-ramp. Where indicated, exogenously purified Dam1 complex (Dam1c) and/or ATP were included in the trapping buffer. **b** Traces of optical trap data for an individual force-clamp event. Gray points show the force applied across the kinetochore-microtubule attachment and green points show the same data after smoothing. The blue trace shows the relative position of a single kinetochore-coupled bead as it tracks with the microtubule tip.

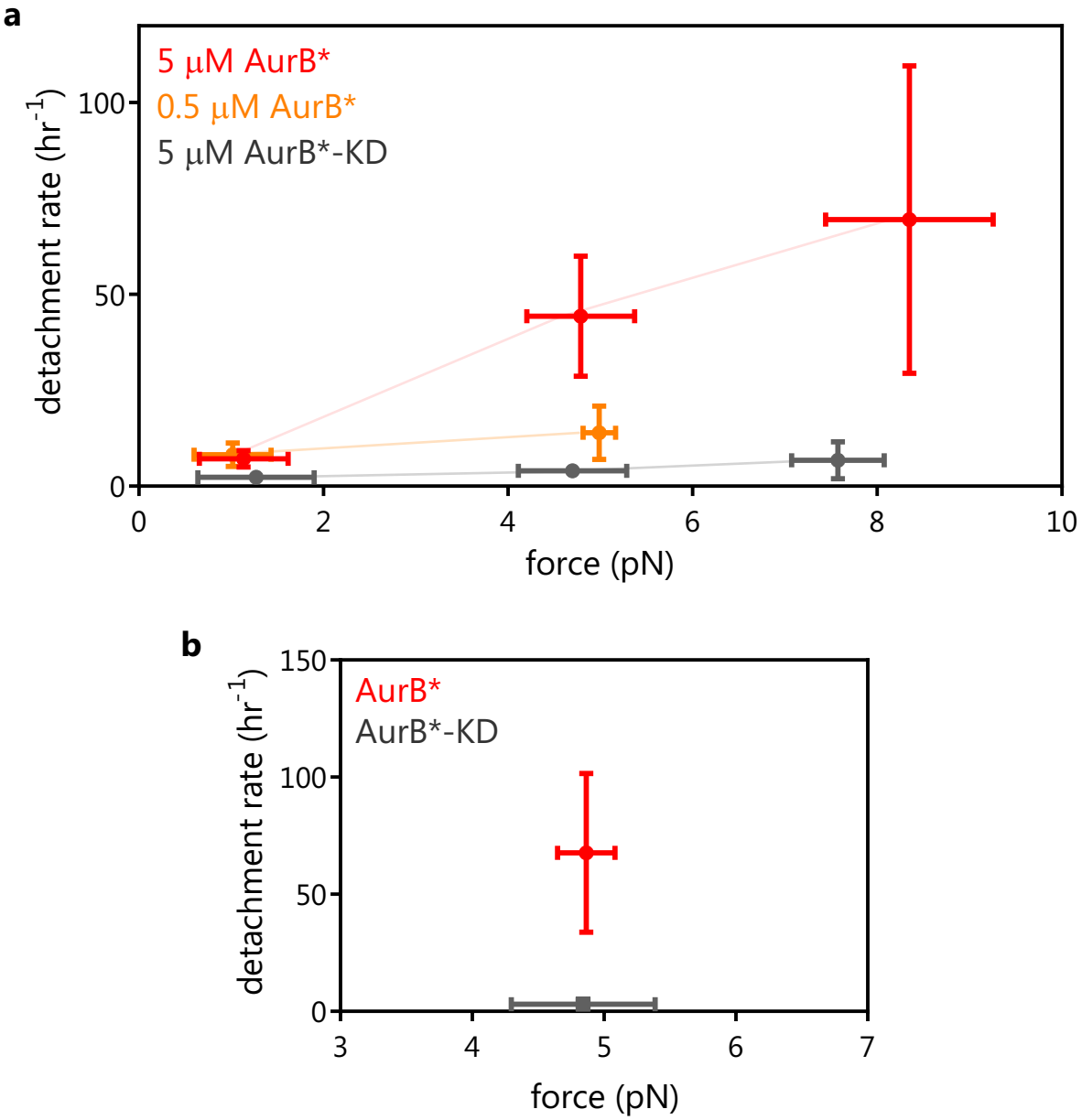

Fig. S4 | **a** Detachment rates for Mps1-1 kinetochores with Dam1 complex present, separated by concentration of kinase. The data at 1 pN and 5 pN are replotted from Figs. 4 and 5. For the data at 8 pN, n = 4 events and 2 detachments (AurB*-KD) or n = 3 events and 3 detachments (5 μM AurB*). **b** Detachment rates for wild-type kinetochores at high force. The assay was performed as diagramed in Fig. 3a, except with wild-type kinetochores and no addition of Dam1 complex. 5 μM of either AurB* or AurB*-KD was flowed in.

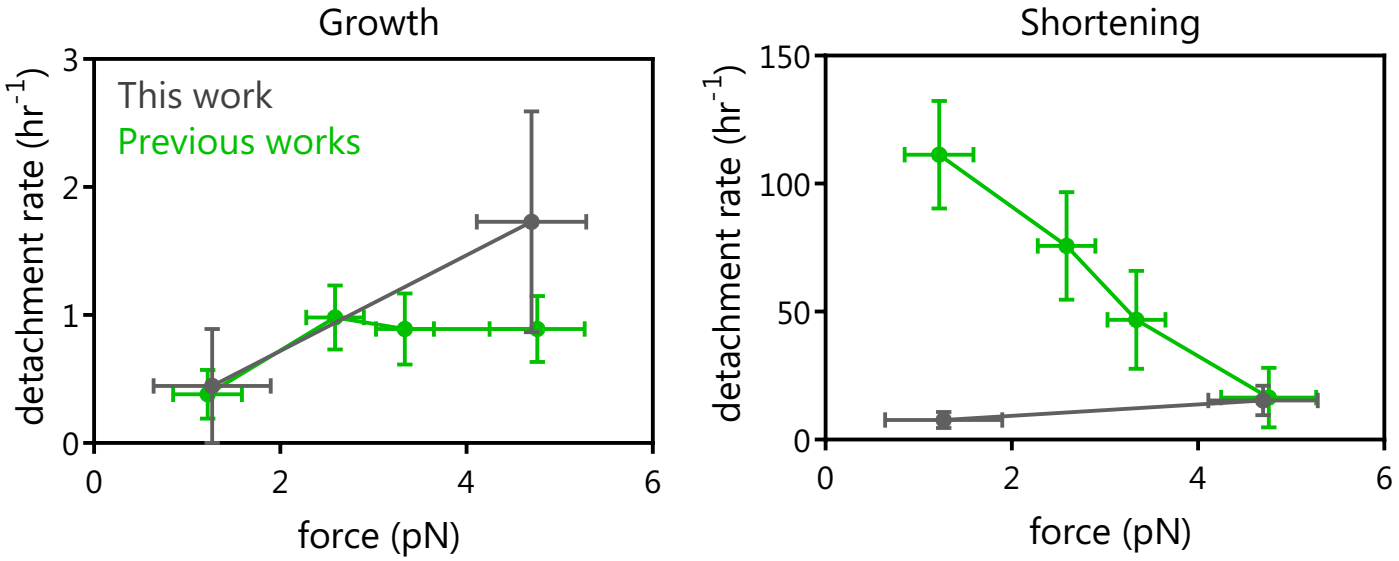

Fig. S5 | a and **b** Kinetochore detachment rates measured specifically during microtubule growth (**a**) and during microtubule shortening (**b**). Rates measured for this work, using Mps1-1 kinetochores with Dam1 complex and AurB*-KD flow, are shown in gray. Rates for wild-type kinetochores, from previous work [41,53], are shown in green.

Tables

Table 1 | Yeast strains used in this study

SBY8253 ***MAT*a** *ura3-1 leu2,3-112 his3-11 trp1-1 ade2-1 LYS2 can1-100 bar1-1 DSN1-6HIS-FLAG::URA3*

SBY8522 ***MAT*a** *ura3-1 leu2,3-112 his3-11 trp1-1 ade2-1 LYS2 can1-100 bar1-1 DSN1-6HIS-3FLAG::URA3 ndc80::NAT::ndc80(T21A,S37A,T54A,T71A,T74A,S95A, S100A)::TRP1*

SBY8726 ***MAT*a** *ura3-1 leu2,3-112 his3-11 trp1-1 ade2-1 LYS2 can1-100 bar1-1 DSN1-6His-3Flag::URA3 mps1-1*

SBY12464 ***MAT*a** *ura3-1 leu2,3-112 his3-11 trp1-1 ade2-1 LYS2 can1-100 bar1-1 DAD1-3Flag::TRP1*

Table 2 | Kinetochore-microtubule detachment rates

flow with	force (pN)	error in force	detachment rate (min^{-1})	error in detachment rate
AurB*-KD	1.27	0.63	2.31	0.87
	4.70	0.59	3.97	1.20
	7.57	0.50	6.76	4.78
5 μM AurB*	1.13	0.48	7.17	2.16
	4.79	0.58	44.3	15.6
	8.35	0.91	69.4	40.1
0.5 μM AurB*	1.02	0.42	8.24	3.11
	4.99	0.18	13.9	6.97
combined AurB*	1.09	0.45	7.57	1.78
	4.84	0.51	25.6	7.41
	8.35	0.91	69.4	40.1

Supplementary Note

Our previous work has shown that tension can directly stabilize reconstituted attachments between kinetochores and dynamic microtubule tips[41,53], but we did not see this "catch bond-like" effect in the present study. We do not know the precise reasons for the difference, but it probably arose from changes in experimental conditions that were implemented here to enable measurement of Aurora-triggered detachments, as detailed below.

The catch bond-like behavior depends on a combination of two effects, tension-dependent suppression of microtubule shortening, and rapid detachment during shortening[41,53]. In the present study, kinetochore detachment during shortening was relatively rare, occurring at a rate of only 7.7 ± 3.1 hr^{-1} at 1 pN of tension, whereas previously it was more frequent, occurring at >100 hr^{-1} at 1 pN (Fig. S5). Thus, the overall release rate in the absence of kinase activity remained relatively low at all forces tested (Figs. 5a, S4a). This behavior fortuitously allowed kinase-triggered release to be detected more readily but eliminated the catch bond-like effect.

Mps1-1 kinetochore particles were used here to avoid the potentially confounding influence of Mps1 kinase, which co-purifies with the wild-type particles used previously. The Mps1-1 kinetochores were bound at a relatively higher density on the beads, to help facilitate microtubule binding during assay setup, and excess free Dam1 was added, to reduce spontaneous detachment. We speculate that one or more of these changes might explain the reduced kinetochore detachment rates during microtubule shortening.